MERGING ASPECTS OF DMO CORRECTION AND CRS STACK TO ACCOUNT FOR CONFLICTING DIP SITUATIONS

M. Soleimani and J. Mann

email: *msoleimani@shahroodut.ac.ir*

keywords: *stacking, diffraction traveltimes, conflicting dips*

ABSTRACT

The Common-Reflection-Surface stack employs a discrete number of stacking operators for the simulation of a particular zero-offset sample: the pragmatic search strategy of the original 2D CRS stack implementation consists of three one-parameter searches. This implementation determines only one optimum stacking operator for each ZO sample to be simulated. Consequently, conflicting dip situations are not taken into account but only the most prominent event contributes to a particular stack sample. Later, the strategy has been extended in order to take into account up to five conflicting dips at each sample. However, the reliable detection of such situations if often difficult and the discrete number of contributions might cause artifacts in the stacked section.

Here, we propose a strategy which explicitely considers all possible angles and, thus, accounts for all the conflicting dips that may exist at each sample. This strategy has some advantages that improve the continuity of events, reflections as well as diffractions, in conflicting dip situations. As it is based on an approximation of diffraction traveltimes, it generally emphasizes diffraction events in the stacked section and can be called common-diffraction-surface stack. This method does not provide wavefield attributes or coherence values, but complements the conventional CRS-stacked section. We processed the Sigsbee 2A synthetic data as well as a real land data set with the new method to demonstrate its ability to handle conflicting dip situations and the favorable effects on a subsequent poststack migration.

INTRODUCTION

The Common-Reflection-Surface (CRS) Stack is a data-driven imaging method to simulate a zero-offset (ZO) section. Introduced by Müller (1998) and Müller et al. (1998) as a ZO simulation method for 2D, it does not require an explicit knowledge of the macro-velocity model. The CRS stack assumes the subsurface to be set up by reflector segments with arbitrary location, orientation, and curvature. Obviously, this subsurface model is more appropriate to describe reflectors in the subsurface than the assumptions inherent to the sequence normal moveout/dip moveout/stack, which is based on ZO isochrone segments in the subsurface. The CRS stacking operator is a second-order approximation of the kinematic reflection response of a curved interface in a laterally inhomogeneous medium. For the 2D case, the shape of the operator depends on three parameters and can be considered as the approximate reflection response of a circular reflector segment in depth, the so-called CRS (Jäger, 1999). Any contributions along any realization of this operator are tested by coherence analysis for each ZO sample, and the set of attributes which yields the highest coherence is accepted as the parameters of the optimum operator to perform the actual stack.

The CRS stack has the potential to sum up more coherent energy of the reflection event which results in a high signal-to-noise ratio (S/N) in the simulated ZO section. However, in each ZO section we could see that in some cases the events intersect each other, e. g. when there are diffraction events which intersect many reflection events with their long tails, or bow tie structures that intersect themselves. Obviously, a single stacking operator associated with only one triplet of optimum attributes is not sufficient in this

conflicting dip situations. Instead, a separate operator is required for each contributing event. To handle conflicting dip situations in the CRS stack without the need for an explicit determination of a discrete number of contributing events, the original search strategy will be adapted and compared to the previous efforts to solve this problem. Finally, the new strategy will be evaluated with synthetic and real data examples.

SEARCH AND STACKING STRATEGIES

In this section we briefly summarize the original pragmatic search strategy for the determination of the CRS stacking parameters, its extended counterpart which handles a discrete number of contributions at each sample, and finally introduce the new concept which enhances diffraction events and fully simulates the superposition of conflicting events.

Pragmatic search strategy

To apply CRS stack in an entirely data oriented way, its attributes have to be determined by means of coherence analysis from prestack data within user-defined attribute ranges. The most efficient solution of the ZO 2D CRS equation

$$t^2\left(x_{\mathrm{m}},h\right)=\left[t_0+\frac{2\sin\alpha}{v_0}\left(x_{\mathrm{m}}-x_0\right)\right]^2+\frac{2t_0\cos^2\alpha}{v_0}\left[\frac{\left(x_{\mathrm{m}}-x_0\right)^2}{R_{\mathrm{N}}}+\frac{h^2}{R_{\mathrm{NIP}}}\right], \tag{1}$$

where R_{NIP} is the radius of normal-incidence-point (NIP) wave, R_{N} is the radius of the normal wave, and α is the emergence angle of the normal ray, can be achieved if it is decomposed into three separate optimization problems with a search for one parameter in each. Müller (1998) and Jäger et al. (2001) describe the complete CRS stack computation routine which involves three one-parameter searches. Optionally, a local optimization with all parameters can be performed afterwards using the flexible polyhedron search method. The pragmatic search strategy can be summarized as follows: automatic CMP stack, linear and hyperbolic ZO stacks, initial CRS stack, and optimization. The first step only considers CMP gathers $(x_{\mathrm{m}}=x_0)$ to determine a combination of R_{NIP} and α (or, in more familiar terms, stacking velocity). In the second step, the simulated ZO section $(h=0)$ of the automatic CMP stack is used to determine α in a linear approximation and R_{N} in a hyperbolic approximation. Finally, the initial stack employs all parameters to perform the stack with the full spatial stacking operator (1).

Extended search strategy

Mann (2001) introduced an extended strategy for CRS stack to address the problem of conflicting dip situations in this method. From the previous strategy, it is clear that this problem can not be handled in the first step, the automatic CMP stack, as stacking velocity analysis is not very sensitive to dip and completely insensitive to its sign. Nevertheless, conflicting dips can be addressed in the second step, ZO stack. Although in the extended strategy the automatic CMP stack is performed without considering conflicting dip situations, its result is used in the next step to resolve the problem of conflicting dips corresponding to different emergence angles α_i. We have to consider more than one CRS operator, according to the number of events that contribute to a particular ZO sample. For that purpose, Mann (2001) considered additional local coherence maxima in the linear ZO stack to identify such situations and to define a discrete number of operators for each particular ZO sample according to absolute and relative coherence thresholds. Once the number of contributing events is known, the determination of their individual attributes α_i and $R_{\mathrm{N},i}$ is straightforward. Wherever conflicting events have been detected, an additional search for the remaining attributes $R_{\mathrm{NIP},i}$ is required. Mann (2002) proposed to use the common shot/common receiver gathers to determine a combined parameter that allows to calculate $R_{\mathrm{NIP},i}$.

The crucial aspect in this extended strategy is the reliable determination of conflicting dip situations. The number of detected contributions might vary along the events and along the wavelets, probably leading to artifacts and/or incomplete superposition of the intersecting events.

Common-diffraction-surface stack strategy

The well-known dip-moveout (DMO) correction (see, e. g. Hale, 1991) corrects for the reflection point dispersal occurring during the normal-moveout (NMO) correction. This is achieved by collecting all contributions for all possible dips (or emergence angles) in the moveout-corrected prestack time domain. In the following we will adopt this by performing CRS stack explicitely for all emergence angles within a given range.

Diffraction events are usually far weaker than reflection events. As a consequence, they strongly suffer from incomplete handling of conflicting dip situations. To enhance diffraction events in addition to the consideration of all plausible dips, we choose a traveltime approximation for diffraction events in the following. For actual diffraction events, the attributes R_{NIP} and R_{N} coincide—exploding reflector experiment and exploding point source are identical in this case. Accordingly, the CRS operator only depends on one remaining parameter $R_{\text{CDS}} = R_{\text{NIP}} = R_{\text{N}}$:

$$t^2_{\text{CDS}}(x_{\text{m}}, h) = \left[t_0 + \frac{2\sin\alpha}{v_0}(x_{\text{m}} - x_0)\right]^2 + \frac{2t_0\cos^2\alpha}{v_0}\frac{(x_{\text{m}} - x_0)^2 + h^2}{R_{\text{CDS}}}. \tag{2}$$

To distinguish this approximation from the full CRS operator (1), we refer to this operator as the common-diffraction-surface (CDS) stack operator. For a *reflection* event, a coherence-based fit of this diffraction operator to the event will yield a radius of curvature R_{CDS} which is a combination of the now independent attributes R_{NIP} and R_{N}. The CDS operator will fit such reflection events worse than diffraction events, thus enhancing the latter. Garabito et al. (2001) applied the same operator in an alternative attribute search scheme with two independent parameters. In contrast, in the approach proposed here, the emergence angle α is predefined and only R_{CDS} remains as free parameter for each fixed angle. The proposed strategy is applied in the prestack time domain and can be briefly summarized as follows:

- for each ZO sample (x_0, t_0)
- for each α, $\alpha_{\text{min}} \leq \alpha \leq \alpha_{\text{max}}$, increment $\Delta\alpha$
- determine R_{CDS} by maximizing coherence along eq. (2)
- stack along optimum operator
- superimpose the contributions for all angles

This strategy is neither suited nor intended to determine CRS wavefield attributes for further applications like inversion. Instead, our aim is to obtain a stacked section which is suited for improved imaging of e. g. faults in a subsequent poststack migration: a sample in the ZO section will receive contributions of any possible optimum operator for each angle that we are searching for. On the one hand, this enhances any weak reflection and diffraction events which were obscured by dominant coherent events in the previous strategy. On the other hand, the multitude of used operators will sum up more incoherent noise than a single CRS operator. Therefore, we expect a lower S/N ratio in the CDS stack results but a better definition of faults and similar structures associated with diffraction events.

The definitions of target zone and aperture are the same as for the pragmatic and extended search strategies (see, e. g., Mann, 2002, for details). The search range for the radius of curvature R_{CDS} can be defined in terms of a generalized stacking velocity similar to the automatic CMP stack. However, the search range of this velocity has to include higher velocities, i. e. smaller moveouts, compared to the usual stacking velocity: the normal wave with its usually smaller curvature and, thus, smaller moveout compared to the NIP wave also contributes to this parameter.

SYNTHETIC DATA EXAMPLE

The Sigsbee 2A data (see, e. g., Pfaffenholz, 2001) are based on a stratified background model containing a salt body with a quite complicated geometry. Figure 1 shows the CRS-stacked section created with the extended search strategy together with the CDS-stacked section according to the proposed approach. In the left part there are slightly dipping layers up to a time of 9 s ending with a strong reflection event. In the

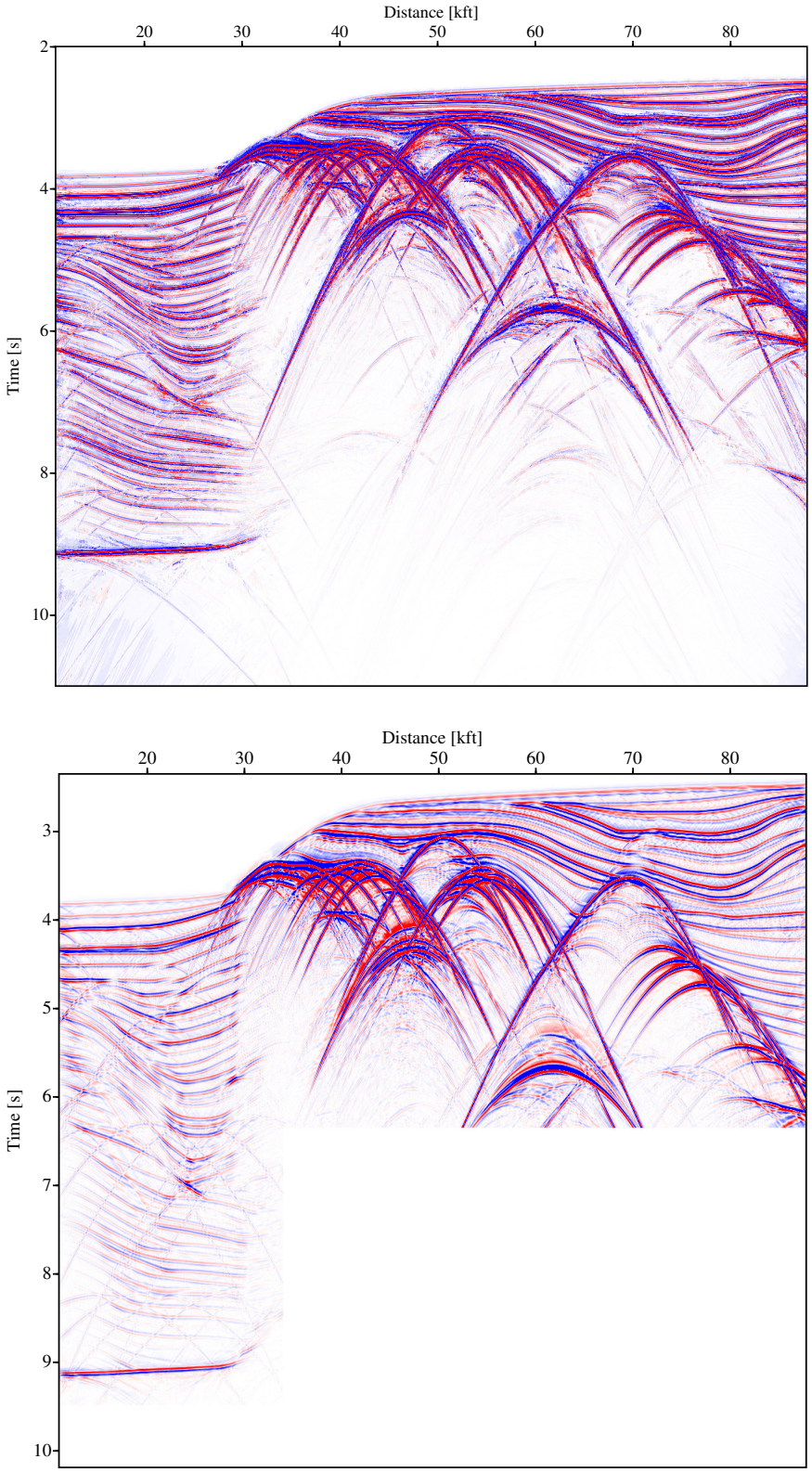

Figure 1: Sigsbee 2A data: CRS-stacked section with up to three dips (top), CDS-stacked section considering all dips (bottom, lower right part has been omitted).

top right part there are also similar sedimentary structures which cover the salt body with its small syncline feature. Strong, extended diffraction patterns dominate the central part of the section whereas some weak diffraction events can also be seen in the left and lower parts of the section.

Compared to the result of the CRS stack, as it could be seen at the first glance, diffraction patterns are enhanced in all parts of the CDS-stacked section. In particular in the sedimentary structures in the left-hand part, diffraction events which are partly or fully obscured by reflection events in the CRS stack section are clearly imaged. There are no gaps or artifacts along such events as all dips are explicitely considered. In the upper part, there are also some diffraction curves in a regular pattern which are most likely due to modeling effects. Note that the lower right part of the CDS section has been omitted during processing to shorten the total computation time.

REAL LAND DATA EXAMPLE

The 2D seismic land dataset was acquired by an energy resource company in a fixed-spread geometry. The seismic line has a total length of about 12 km. The utilized source signal was a linear upsweep from 12 to 100 Hz of 10 s duration. Shot and receiver spacing are both 50 m and the temporal sampling interval is 2 ms. Standard preprocessing was applied to the field data including the setup of the data geometry, trace editing, deconvolution, geometrical spreading correction, field static correction, and bandpass filtering. The underlying structure consists of nearly horizontally layers and some dipping layers due to dip faulting in some parts.

In CRS stack processing, mapping the position of faults, their boundaries, and their orientations is difficult because the problem of conflicting dips also exists here at the end points of faults and also where the layers are faulted. The energy lacking due to undetected diffraction events leads to incomplete focusing of the faults in a subsequent poststack migration.

Figure 2 shows the stacked sections of the CRS procedure and the CDS results for these data. As expected the overall S/N ratio is lower in the CDS-stacked section. Diffraction events are again emphasized but that is not as obvious from the stacked section itself.

A macro-velocity model for this data was available from NIP wave tomography (see, e. g., Hertweck et al., 2004) such that poststack depth migration can be applied to compare the result with the result of the migrated CRS-stacked section. The Greens functions tables for depth migration were calculated using an eikonal solver and migration has been done with a Kirchhoff algorithm. Figure 3 shows the migration results of the two different stack sections (Figure 2). Although the S/N ratio is slightly lower in the migrated CDS section, the faults are better defined than in the migrated CRS section.

CONCLUSIONS AND OUTLOOK

The pragmatic approach of Müller (1998) and the extended strategy of Mann (2002) have been combined with the concepts of DMO correction to overcome the problem of conflicting dip situations. In this approach not only a few selected dips are selected and assigned with an stacking operator, but all angles within a predefined range are considered, each with a separate operator for each sample. In addition, an traveltime approximation for diffraction events is used to enhance such usually weak events and to reduce computational costs. The search for the only remaining attribute R_{CDS} is performed in one step in the prestack time domain rather than in selected subdomains.

The stack result for synthetic and real data indicate that this strategy fully resolves conflicting dip situations and enhances diffraction events and other weak events previously obscured by strong reflection events. The results of poststack depth migration of a real data set demonstrates that the stacked section of the CDS stack is well suited as input for poststack migration. The new strategy collects more energy that might be lost in the previous strategies. This leads to an improved image quality especially at discontinuities and in faulted areas which, in turn, improves the migration result. Thus, the CDS-based results with their better imaged and focused diffraction events complement the conventional CRS results with their higher S/N ratio.

The future development of the CDS stack method will focus on the automated selection of the angle search ranges. Currently, the same (large) angle range is used irrespective of the local situation. On the one hand, this guarantees that all potential dips can contribute. On the other hand, this slows down the process and decreases the S/N ratio. A smart selection strategy might ease this problems without impairing the

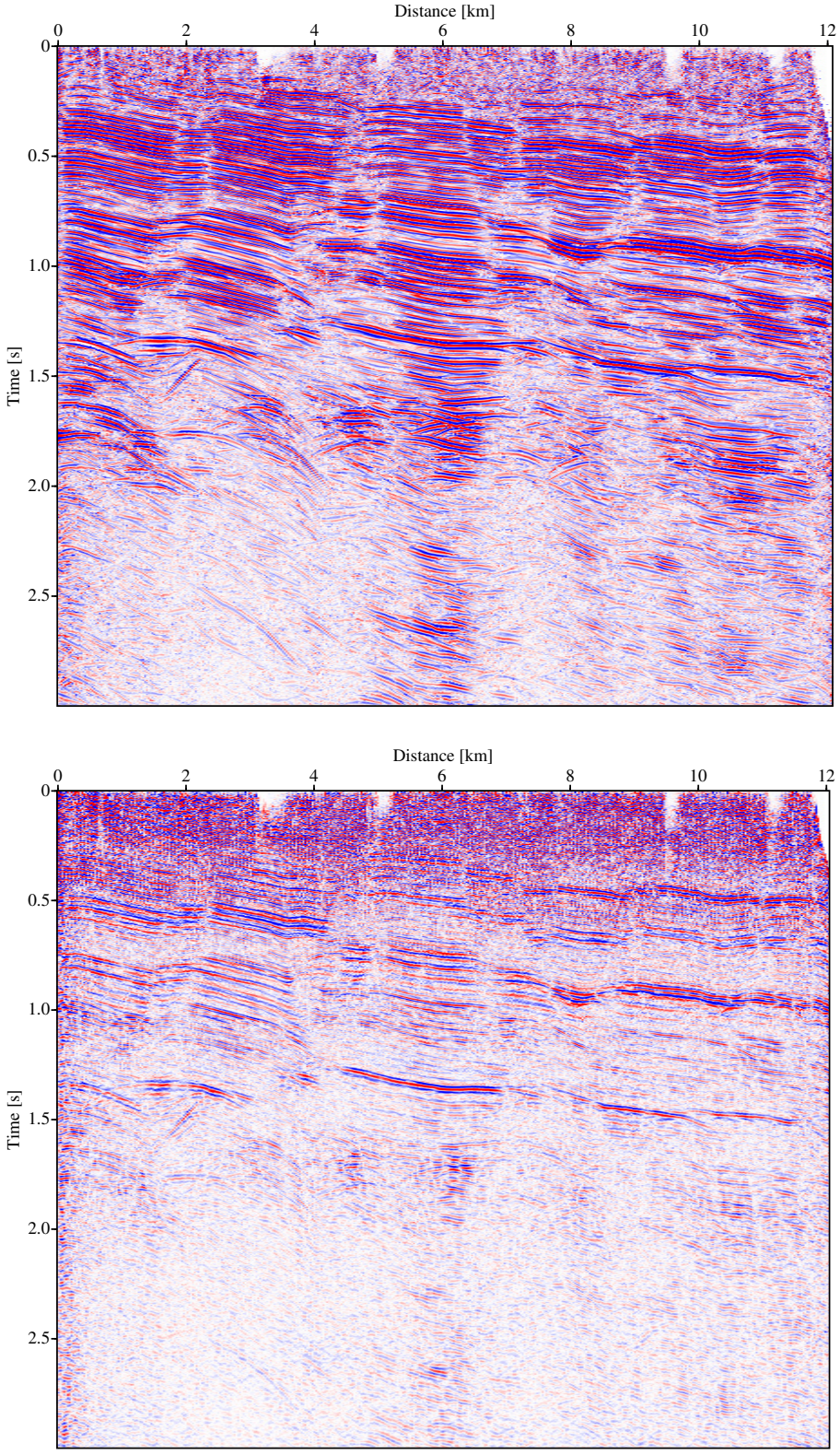

Figure 2: Real land data: CRS-stacked section with up to three dips (top), CDS-stacked section considering all dips (bottom).

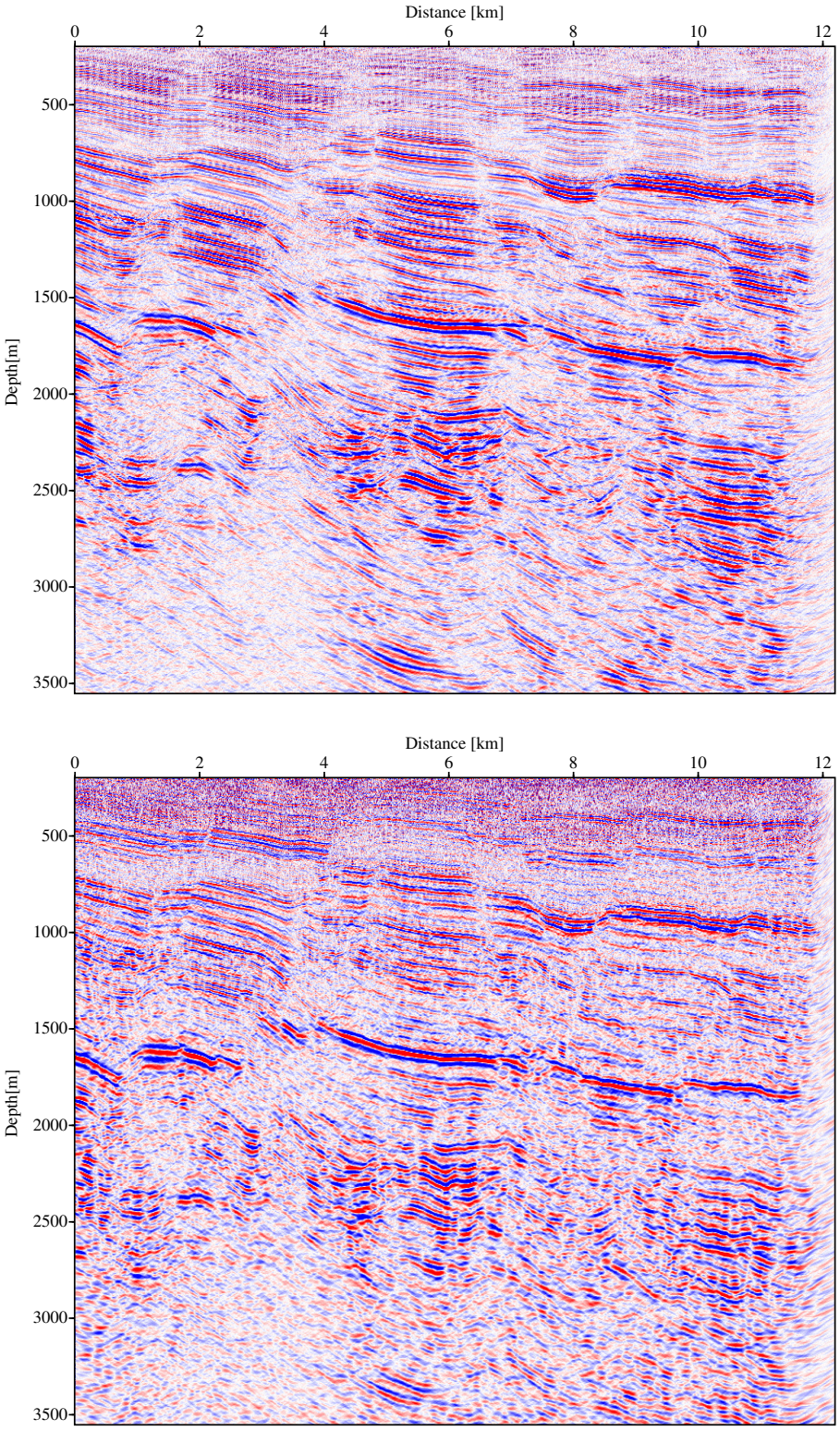

Figure 3: Real land data: poststack migrations results of CRS-stacked section (top) and CDS-stacked section (bottom).

weak events to be enhanced.

REFERENCES

Garabito, G., Cruz, J. C. R., Hubral, P., and Costa, J. (2001). Common reflection surface stack: a new parameter search strategy by global optimization. In *Ann. Report*, volume 4, pages 35–48. Wave Inversion Technology Consortium.

Hale, D. (1991). *Dip Moveout Processing*. Soc. Expl. Geophys., Tulsa.

Hertweck, T., Jäger, C., Mann, J., Duveneck, E., and Heilmann, Z. (2004). A seismic reflection imaging workflow based on the Common-Reflection-Surface (CRS) stack: theoretical background and case study. In *Expanded Abstract, 74th Ann. Internat. Mtg.* Soc. Expl. Geophys. Session SP 4.3.

Jäger, R. (1999). The Common Reflection Surface stack – theory and application. Master's thesis, University of Karlsruhe.

Jäger, R., Mann, J., Höcht, G., and Hubral, P. (2001). Common-Reflection-Surface stack: image and attributes. *Geophysics*, 66(1):97–109.

Mann, J. (2001). Common-Reflection-Surface stack and conflicting dips. In *Extended abstracts, 63rd Conf.* Eur. Assn. Geosci. Eng. Session P077.

Mann, J. (2002). *Extensions and applications of the Common-Reflection-Surface Stack method*. Logos Verlag, Berlin.

Müller, T. (1998). Common Reflection Surface stack versus NMO/stack and NMO/DMO/stack. In *Extended abstracts, 60th Conf.* Eur. Assn. Geosci. Eng. Session 1-20.

Müller, T., Jäger, R., and Höcht, G. (1998). Common Reflection Surface stacking method – imaging with an unknown velocity model. In *Expanded abstracts, 68th Ann. Internat. Mtg.*, pages 1764–1767. Soc. Expl. Geophys.

Pfaffenholz, J. (2001). Sigsbee2 synthetic subsalt data set: image quality as function of migration algorithm and velocity model error. In *Workshop on velocity model independent imaging for complex media, Extended abstracts*. Soc. Expl. Geophys. Session W5-5.